Hindawi
International Journal of Aerospace Engineering
Volume 2019, Article ID 3139204, 11 pages
https://doi.org/10.1155/2019/3139204

Research Article

Propulsion and Thermodynamic Parameters of van der Waals Gases in Rocket Nozzles

Fernando S. Costa and Gustavo A. A. Fischer

Combustion and Propulsion Laboratory, National Institute for Space Research, Cachoeira Paulista, SP 12.630-000, Brazil

Correspondence should be addressed to Gustavo A. A. Fischer; gustavo.achilles.fischer@gmail.com

Received 31 January 2019; Revised 21 June 2019; Accepted 4 July 2019; Published 14 August 2019

Academic Editor: Jose Carlos Páscoa

Propellants or combustion products can reach high pressures and temperatures in advanced or conventional propulsion systems. Variations in flow properties and the effects of real gases along a nozzle can become significant and influence the calculation of propulsion and thermodynamic parameters used in performance analysis and design of rockets. This work derives new analytical solutions for propulsion parameters, considering gases obeying the van der Waals equation of state with specific heats varying with pressure and temperature. Steady isentropic one-dimensional flows through a nozzle are assumed for the determination of specific impulse, characteristic velocity, thrust coefficient, critical flow constant, and exit and throat flow properties of He, H_2, N_2, H_2O, and CO_2 gases. Errors of ideal gas solutions for calorically perfect and thermally perfect gases are determined with respect to van der Waals gases, for chamber temperatures varying from 1000 to 4000 K and chamber pressures from 5 to 35 MPa. The effects of covolumes and intermolecular attraction forces on flow and propulsion parameters are analyzed.

1. Introduction

The classical equations for the calculation of rocket propulsion parameters are based on one-dimensional flows of ideal gases with constant properties [1]. The NASA CEA (Chemical Equilibrium and Applications) code is largely used for the preliminary design of rockets and calculates nozzle properties and propulsion parameters considering frozen or equilibrium one-dimensional flows of thermally perfect ideal gases [2]. Nevertheless, propellants and combustion products in advanced or conventional propulsion systems, such as electrothermal, microwave, laser, nuclear, and chemical rockets, can attain relatively high temperatures and pressures [3–6]. In general, at elevated temperatures, the effects of molecular attraction are negligible and compressibility factors of fluids are close to unity. However, pressures and temperatures decrease rapidly and at different rates along the nozzle, and consequently, real gas effects and variations of properties can become significant. Chamber conditions also can be affected by real gas behavior, such as equilibrium composition and temperature, reaction rates, and other combustion parameters, especially at high pressures [7, 8]. Other processes can affect the performance of nozzles and propulsion parameters, such as viscous losses, chemical kinetics, heat transfer, boundary layer, flow separation, shock waves, two-phase flow, and three-dimensional effects [9–13]. Correction factors are often used to estimate the performance of real nozzles; however, there is limited information about the effects of real gases and variable properties.

The main propulsion parameters used to evaluate performance characteristics of rockets are specific impulse, characteristic velocity, and thrust coefficient. Specific impulse relates the total impulse to the total weight of a burned or ejected propellant. The characteristic velocity is a measure of propellant performance and motor design quality, whereas the thrust coefficient indicates nozzle design efficiency. Another important parameter, mainly used for a nozzle design, is the critical flow constant which determines the mass flow rate from chamber stagnation conditions [1].

Several studies have considered one-dimensional flows of perfect gases or imperfect gases with variable properties in nozzles, in general without focusing on the determination of propulsion parameters. Johnson [14] investigated the effects of real gases on the critical flow constant, using virial

Table 1: van der Waals constants.

	He	H_2	N_2	H_2O	CO_2
T_{cr} (K)	5.19	33.18	126.10	647.13	304.19
P_{cr} (MPa)	0.23	1.31	3.39	22.06	7.38
$a = 27(RT_{cr})^2/64P_{cr}$ (Pa·m^6·kg^{-2})	215.9	6016.8	174.1	1706.3	188.7
$b = RT_{cr}/8P_{cr}$ (m^3/kg)	0.0059	0.0130	0.0014	0.0017	0.0010

equations based on curve fits of thermodynamic tables. Critical flow constants were determined for air, N_2, O_2, normal-H_2, para-H_2, and steam; for temperatures 389-833 K; and for pressures 0-300 atm. Witte and Tatum [15] developed a computer code to determine thermally ideal gas properties, using specific heats approximated as NASA fourth-order polynomials of the temperature. The AGARD-AR-321 report [16] presented real gas discharge coefficients, based on experimental and numerical data from Masure and Johnson, in order to correct the mass flow rate and thrust in air nozzles for stagnation temperatures up to 344 K and stagnation pressures up to 100 bar, and the results were then compared to calorically perfect ideal gas solutions. Kim et al. [17] investigated the flow of high-pressure hydrogen gas through a critical nozzle, using the Redlich-Kwong equation of state with the axisymmetric, compressible Navier-Stokes equations to account for the intermolecular forces and molecular volume of hydrogen. They verified that the critical pressure ratio and the discharge coefficient for the ideal gas assumption are significantly different from those of the real gas, as the Reynolds number happens to exceed a certain value. Yoder et al. [18] have made numerical simulations of air flow through a nozzle assuming calorically perfect air, a calorically perfect gas mixture, and a frozen gas mixture. Thus, they have managed to determine performance parameters such as mass flow rate, gross thrust, and thrust coefficient. Górski and Rabczak [19] have compared experimental data with theoretical results of the critical flow constant for dense gases. The 1D nonlinear model used parameters of the isentropic flow of real gases, analogous to an ideal gas flow. Nagao et al. [20] have investigated the real gas effects on discharge coefficient and thermodynamics properties through a critical nozzle by using H_2, N_2, CH_4, and CO_2, with the help of a CFD method. Ding et al. [21] have adopted equations of state based on the Helmholtz energy to describe the flow of hydrogen through a critical nozzle and compared theoretical results with experimental data and CFD simulations with different equations of state. Costa [22] has investigated propulsion parameters of Noble-Abel gases and verified that covolume and variation of specific heats with temperature can influence significantly the propulsion parameters, depending on the pressures and temperatures considered.

The present work extends previous studies and derives new analytical solutions for rocket propulsion parameters and nozzle flow thermodynamic parameters of real gases obeying the van der Waals equation of state and provides data for a broad range of stagnation pressures and temperatures. The effects of covolumes and intermolecular attraction forces are analyzed, and the percent errors of propulsion parameters and flow thermodynamic properties of calorically perfect and thermally perfect ideal gases are calculated with respect to van der Waals gases. Steady isentropic one-dimensional frozen flows of He, H_2, N_2, H_2O, and CO_2 are considered for vacuum expansion with chamber temperatures 1000-4000 K, chamber pressures 5-35 MPa, and nozzle expansion ratios 50-200. At high pressures, the specific heats are assumed to depend on pressure and temperature, whereas at low pressures they are calculated based on fourth-order polynomials of temperature [23], as adopted by NASA CEA code [2]. These low pressure-specific heats are adjusted from experimental and theoretical data from different sources, for temperatures from 0 to 20000 K. Lower temperatures (1000-2500 K) are usually reached in electrothermal and catalytic augmented thrusters while higher temperatures (2500-4000 K) can be attained in chemical and nuclear rockets.

2. Theoretical Analysis

The van der Waals equation of state (VDW EOS) has the following form:

$$\left(P + \frac{a}{v^2}\right)(v - b) = RT, \tag{1}$$

where P is the pressure, T is the temperature, v is the specific volume, R is the specific gas constant, a is the coefficient for intermolecular attraction, and b is the covolume, an effective molecular volume. Constants a and b are, in general, determined in terms of critical constants, as presented in Table 1. Alternatively, these constants can be determined by curve fits of experimental data or from more accurate equations of state for specific ranges of pressure and temperature. Nevertheless, experimental data for fluids at high pressures are, in general, limited to temperatures lower than 2000 K [24]. In the case of mixtures of propellants or combustion products, the VDW constants a and b can be estimated from $\sqrt{a} = \sum X_i \sqrt{a_i}$ and $\sqrt{b} = \sum X_i \sqrt{b_i}$, where X_i is the molar fractions of propellant/product i or can be estimated from pseudocritical constants, as described by Walas [25]. Maximum densities considered in this work are far from the critical density values, where the van der Waals equation is less accurate. Table 2 shows the maximum and critical densities.

It is worth mentioning that the adoption of more accurate and detailed equations of state, using attraction parameters dependent on temperatures, would require full numerical solutions in order to determine the propulsion and thermodynamic parameters.

Table 2: Maximum densities (1000 K and 35 MPa) and critical densities (Data from [24]).

	He	H_2	N_2	H_2O	CO_2
ρ_{max} (kg/m^3)	16.9	7.95	104.92	83.25	170.60
ρ_{cr} (kg/m^3)	69.64	31.26	313.30	322.00	467.60

The evaluation of thermodynamic properties is required for the derivation of analytical solutions for the flow properties and propulsion parameters. Initially, the specific heats of a real gas at constant pressure and volume, c_p and c_v, respectively, are obtained from the thermodynamic relations:

$$c_v - c_v^0 = T\int_0^v \left(\frac{\partial^2 P}{\partial T^2}\right)_v dv, \tag{2}$$

$$c_p - c_v = T\left(\frac{\partial v}{\partial T}\right)_P \left(\frac{\partial P}{\partial T}\right)_v, \tag{3}$$

where the "0" superscript denotes ideal gas property. Replacing equation (1) into equations (2) and (3) provides $c_v = c_v^0$ and $c_p - c_v = R/(1-\Delta)$ with

$$\Delta = \frac{2\varepsilon}{1+\varepsilon}(1-b^*) < 1, \tag{4}$$

where $b^* = b/v$ and $\varepsilon = a/(Pv^2)$ are, respectively, the nondimensional covolume and nondimensional attraction parameter. Consequently, $c_p > c_v$ and the ratio of specific heats, $\gamma = c_p/c_v$, of a VDW gas are

$$\gamma = \frac{\gamma^0 - \Delta}{1-\Delta} > \gamma^0 = \frac{c_p^0}{c_v^0}. \tag{5}$$

A differential entropy variation ds can be calculated from

$$ds = c_v\frac{dT}{T} + \left(\frac{\partial P}{\partial T}\right)_v dv = c_v^0\frac{dT}{T} + R\frac{d(v-b)}{v-b}. \tag{6}$$

Considering an isentropic process, $ds = 0$, and using $c_p^0 - c_v^0 = R$, the integration of equation (6) yields the variation of a specific volume:

$$\frac{v-b}{v_c-b} = \frac{T}{T_c}\exp\left(\int_T^{T_c}\frac{c_p^0}{R}\frac{dT}{T}\right), \tag{7}$$

where subscript "c" denotes chamber conditions. Combining equations (1) and (7), the pressure variation along the nozzle is determined:

$$\frac{P + a/v^2}{P_c + a/v_c^2} = \exp\left(-\int_T^{T_c}\frac{c_p^0}{R}\frac{dT}{T}\right). \tag{8}$$

A differential enthalpy change dh can be obtained from

$$dh = c_v dT + \left[T\left(\frac{\partial P}{\partial T}\right)_v - P\right]dv + d(Pv). \tag{9}$$

Then, integrating equation (9) from $h_1(T_1, v_1)$ to $h_2(T_2, v_2)$ yields

$$h_2 - h_1 = \int_{T_1}^{T_2}\left(c_p^0 - R\right)dT + \frac{a}{v_1} - \frac{a}{v_2} + P_2v_2 - P_1v_1, \tag{10}$$

which is similar to the enthalpy equation presented by Cramer and Sen [26].

Flow velocity is calculated from the energy equation $u^2 = 2(h_c - h)$ for steady one-dimensional adiabatic flow with no work performed and no potential energy variation. Consequently, substituting equation (10), it results the following:

$$u = \left\{2\left[\int_T^{T_c} c_p^0 dT + \frac{bRT_c}{v_c - b} - \frac{bRT}{v-b} - \frac{2a}{v_c} + \frac{2a}{v}\right]\right\}^{1/2}. \tag{11}$$

Assuming small pressure variations, the speed of sound is given by $c = [(\partial P/\partial\rho)_s]^{1/2}$ where subscript "s" denotes the constant entropy. Applying Maxwell thermodynamic relations, it follows that

$$u_s = \left[-\gamma v^2\left(\frac{\partial P}{\partial v}\right)_T\right]^{1/2}, \tag{12}$$

and for the VDW EOS, it yields

$$u_{s,\mathrm{VDW}} = \left[\frac{\gamma RT}{(1-b/v)^2} - \frac{2a\gamma}{v}\right]^{1/2}. \tag{13}$$

Equation (13) shows that larger covolumes and smaller intermolecular forces increase the speed of sound. Combining the differential forms of the mass conservation equation and Euler equation, with the speed of sound definition, implies that flow velocity and speed of sound are equal at the nozzle throat:

$$u_t = u_{s,t}, \tag{14}$$

where subscript "t" indicates the throat conditions. Replacing equations (11) and (13) into equation (14) yields the nozzle throat temperature:

$$T_t = \frac{(1-b/v_t)^2}{R}\left\{\frac{2}{\gamma_t}\left[\int_{T_t}^{T_c} c_p^0 dT + \frac{bRT_c}{v_c - b} - \frac{bRT_t}{v_t - b} - \frac{2a}{v_c} + \frac{2a}{v_t}\right] + \frac{2a}{v_t}\right\}, \tag{15}$$

which can be solved iteratively using equation (7) for a specific volume calculated at the nozzle throat. Equation

(15) is significantly simplified for a Noble-Abel (NA) gas, i.e., with $a = 0$ or $\varepsilon = 0$:

$$T_t = \frac{(1 - b_t^*)^2}{R}\left\{\frac{2}{\gamma_t}\left[\int_{T_t}^{T_c} c_p^0 dT + b(P_c - P_t)\right]\right\}, \tag{16}$$

and in the case of thermally perfect ideal gases, $a = b = 0$; therefore, $T_t = (2/\gamma_t)[\int_{T_t}^{T_c}(c_p^0/R)dT]$.

After throat conditions are determined, the critical mass flow rate constant can be calculated: $\Gamma = \dot{m}\sqrt{RT_c}/(A_t P_c)$, where $\dot{m}$ is the mass flow rate of propellants. Since, at the nozzle throat, $\dot{m} = \rho_t u_t A_t = u_{s,t} A_t / v_t$, then,

$$\Gamma_{\mathrm{VDW}} = \left[\gamma_t\left(\frac{RT_t}{(v_t - b)^2} - \frac{2a}{v_t^3}\right)\right]^{1/2}\frac{\sqrt{RT_c}}{P_c}. \tag{17}$$

Defining the characteristic velocity of propellants by $c^* = P_c A_t/\dot{m}$ and replacing equation (17), for a VDW gas, it yields

$$c^*_{\mathrm{VDW}} = \frac{\sqrt{RT_c}}{\Gamma_{\mathrm{VDW}}} \tag{18}$$

The thrust coefficient is defined by $c_F = F/(P_c A_t)$, where F is the rocket thrust. Assuming no divergence losses, $F = \dot{m}u_e + (P_e - P_a)A_e$, where subscript "$e$" denotes the nozzle exit conditions and subscript "a" denotes the ambient conditions. Once the mass flow rate is calculated by

$$\dot{m} = \Gamma A_t \frac{P_c}{\sqrt{RT_c}} \tag{19}$$

and the exit velocity of propellants, or combustion products, is obtained from equation (11), then

$$c_F = \frac{\Gamma}{\sqrt{RT_c}}u_e + \left(\frac{P_e}{P_c} - \frac{P_a}{P_c}\right)\frac{A_e}{A_t}. \tag{20}$$

The exit pressure P_e depends on the nozzle area ratio A_e/A_t, since $\dot{m} = \Gamma A_t P_c/\sqrt{RT_c} = u_e A_e/v_e$ which yields

$$\frac{A_e}{A_t} = \Gamma_{\mathrm{VDW}}\frac{P_c}{\sqrt{RT_c}}\frac{v_e}{u_e}. \tag{21}$$

Therefore, the thrust coefficient of a VDW gas is

$$c_{F,\mathrm{VDW}} = \frac{\Gamma_{\mathrm{VDW}}}{\sqrt{RT_c}}\left[u_e + (P_e - P_a)\frac{v_e}{u_e}\right], \tag{22}$$

where

$$v_e = b + (v_c - b)\frac{T_e}{T_c}\exp\left(\int_{T_e}^{T_c}\frac{c_p^0}{R}dT\right), \tag{23}$$

$$P_e = -\frac{a}{v_e^2} + \left(P_c + \frac{a}{v_c^2}\right)\exp\left(-\int_{T_e}^{T_c}\frac{c_p^0}{R}dT\right), \tag{24}$$

$$u_e = \left\{2\left[\int_{T_e}^{T_c} c_p^0 dT + \frac{bRT_c}{v_c - b} - \frac{bRT_e}{v_e - b} - \frac{2a}{v_c} + \frac{2a}{v_e}\right]\right\}^{1/2}. \tag{25}$$

Exit specific volume, exit pressure, and exit velocity can be calculated for a given exit temperature. Assuming perfect expansion in vacuum, the exit-specific volume will approach infinity, and exit pressure and exit temperature will approach zero; then the optimum thrust coefficient in vacuum can be calculated by

$$c_{F,\mathrm{VDW,opt}} = \frac{\Gamma_{\mathrm{VDW}}}{\sqrt{RT_c}}\left\{2\left[\int_0^{T_c} c_p^0 dT + \frac{bRT_c}{v_c - b} - \frac{2a}{v_c}\right]\right\}^{1/2}. \tag{26}$$

The specific impulse of a rocket is defined by $\mathrm{Isp} = F/(\dot{m}g_o)$, where g_o is the standard gravity acceleration at a sea level. Since $\mathrm{Isp} = c^* c_F/g_o$, the optimum specific impulse in vacuum is

$$\begin{aligned}\mathrm{Isp}_{\mathrm{VDW,opt}} &= \frac{c^*_{\mathrm{VDW}} c_{F,\mathrm{VDW,opt}}}{g_o} \\ &= \frac{1}{g_o}\left\{2\left[\int_0^{T_c} c_p^0 dT + \frac{bRT_c}{v_c - b} - \frac{2a}{v_c}\right]\right\}^{1/2}.\end{aligned} \tag{27}$$

Equation (27) indicates that larger covolumes and smaller intermolecular attraction forces increase the optimum specific impulse, if their influences on specific heat and combustion temperature can be neglected.

3. Simplified Solutions

The previous analytical solutions can be simplified in special cases. The critical flow constant and characteristic velocity of a thermally perfect NA gas [22] are calculated, respectively, by

$$\begin{aligned}\Gamma_{\mathrm{NA}} &= \sqrt{\gamma_{t,\mathrm{NA}}\frac{T_c}{T_{t,\mathrm{NA}}}}\exp\left(-\int_{T_{t,\mathrm{NA}}}^{T_c}\frac{c_p^0}{R}dT\right), \\ c^*_{\mathrm{NA}} &= \sqrt{RT_c}/\Gamma_{\mathrm{NA}},\end{aligned} \tag{28}$$

where $\gamma_{\mathrm{NA}} = c_p^0/c_v^0$ and $\gamma_{t,\mathrm{NA}} = c_p^0(T_{t,\mathrm{NA}})/c_v^0(T_{t,\mathrm{NA}})$. Simplifying equation (20)–(25) yields the thrust coefficient and nozzle area expansion ratio of a rocket propelled by a NA gas:

$$\begin{aligned}c_{F,\mathrm{NA}} &= \Gamma_{\mathrm{NA}}\sqrt{\frac{2}{T_c}\left[\int_{T_e}^{T_c}\frac{c_p^0}{R}dT + \frac{b}{R}(P_c - P_e)\right]} + \left(\frac{P_e}{P_c} - \frac{P_a}{P_c}\right)\frac{A_e}{A_t}, \\ \frac{A_e}{A_t} &= \frac{\Gamma_{\mathrm{NA}}((bP_c/RT_c) + (T_e/T_c)(P_c/P_e))}{\sqrt{(2/T_c)\left[\int_{T_e}^{T_c}\left(c_p^0/R\right)dT + 2(bP_c/RT_c)(1 - (P_e/P_c))\right]}}.\end{aligned} \tag{29}$$

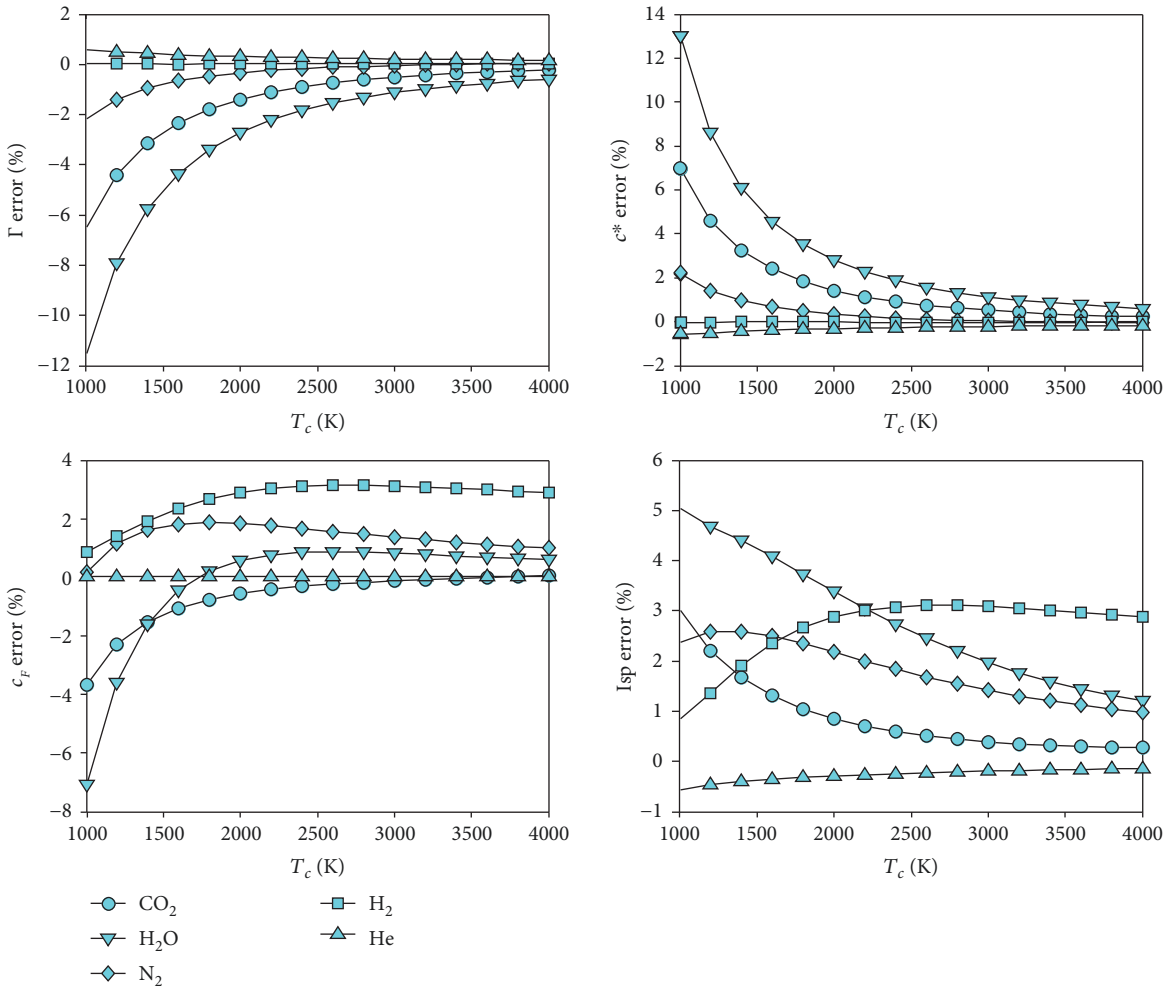

Figure 1: Errors of propulsion parameters of calorically perfect ideal gases with respect to VDW gases at different chamber temperatures, for vacuum expansion, $A_e/A_t = 100$ and $P_c = 10$ MPa.

Since $\mathrm{Isp}_{\mathrm{NA}} = c^*_{\mathrm{NA}} c_{F,\mathrm{NA}}/g_o$, the optimum thrust coefficient and the optimum specific impulse, for a NA gas, are given, respectively, by

$$c_{F,\mathrm{NA,opt}} = \Gamma_{\mathrm{NA}} \sqrt{\frac{2}{T_c}\left[\int_0^{T_c} \frac{c_p^0}{R}\,dT + \frac{bP_c}{R}\right]},$$
$$\mathrm{Isp}_{\mathrm{NA,opt}} = \frac{c^*_{\mathrm{NA}} c_{F,\mathrm{NA,opt}}}{g_o} = \frac{1}{g_o}\sqrt{2\left[\int_0^{T_c} c_p^0\,dT + bP_c\right]}. \quad (30)$$

If intermolecular attraction forces and covolumes are neglected, $a = 0$ and $b = 0$, and the VDW EOS becomes the thermally perfect ideal gas equation of state (IG-TP EOS) and the previous results for NA gases are further simplified. Assuming constant specific heats, calorically perfect solutions for NA gases and ideal gases can be derived.

4. Results and Discussion

Rocket propulsion parameters and flow thermodynamic properties for different rocket chamber conditions and nozzle expansion ratios were obtained for vacuum expansion. Steady isentropic one-dimensional frozen flows of He, H_2, N_2, CO_2, H_2O, and gases following the VDW EOS were considered. Frozen flows are assumed when flow residence time in a nozzle is shorter than reaction times, whereas equilibrium flows require a longer residence time. In the case of hydrogen recombination kinetics, the losses of specific impulses decrease with increasing pressures [9].

At low pressures, the specific heats were assumed to obey fourth-order polynomials of temperature [23] with coefficients a_i, $i = 1, \cdots, 7$:

$$\frac{c_p^0}{R} = a_1 T^{-2} + a_2 T^{-1} + a_3 + a_4 T + a_5 T^2 + a_6 T^3 + a_7 T^4. \quad (31)$$

The percent errors of propulsion parameters $\varnothing = \mathrm{Isp}, \Gamma$, etc. of calorically perfect (CP) and thermally perfect (TP) ideal gases (IG) in relation to VDW gases were calculated from

$$\varepsilon_{\varnothing} = 100\,\frac{\varnothing_{\mathrm{IG}} - \varnothing_{\mathrm{VDW}}}{\varnothing_{\mathrm{VDW}}}. \quad (32)$$

Table 3: Maximum and minimum error values of propulsion and flow parameters of calorically perfect ideal gases for $P_c = 10$ MPa, $T_c = 1000$ K–4000 K and frozen flow expansion in vacuum with $A_e/A_t = 100$.

ϕ	ε_{max} (%)					ε_{min} (%)				
	CO_2	H_2O	N_2	H_2	He	CO_2	H_2O	N_2	H_2	He
Γ	−0.227	−0.590	0.032	0.033	0.590	−6.496	−11.528	−2.152	0.008	0.165
c^*	6.947	13.023	2.200	−0.008	−0.165	0.227	0.593	−0.032	−0.033	−0.587
c_F	0.049	0.870	1.872	3.142	0.034	−3.682	−7.074	0.163	0.874	0.020
Isp	3.010	5.029	2.607	3.111	−0.144	0.277	1.204	0.973	0.847	−0.560
P_e	43.649	51.564	42.491	48.689	2.067	4.672	16.104	21.983	26.396	0.456
M_e	−1.157	−3.806	−5.676	−8.822	−0.236	−8.669	−12.403	−12.172	−13.369	−0.966
P_t	0.536	0.361	1.454	1.117	0.844	0.273	0.047	0.357	0.506	0.213
T_t	0.418	0.744	0.722	0.560	0.339	0.067	0.093	0.127	0.263	0.085

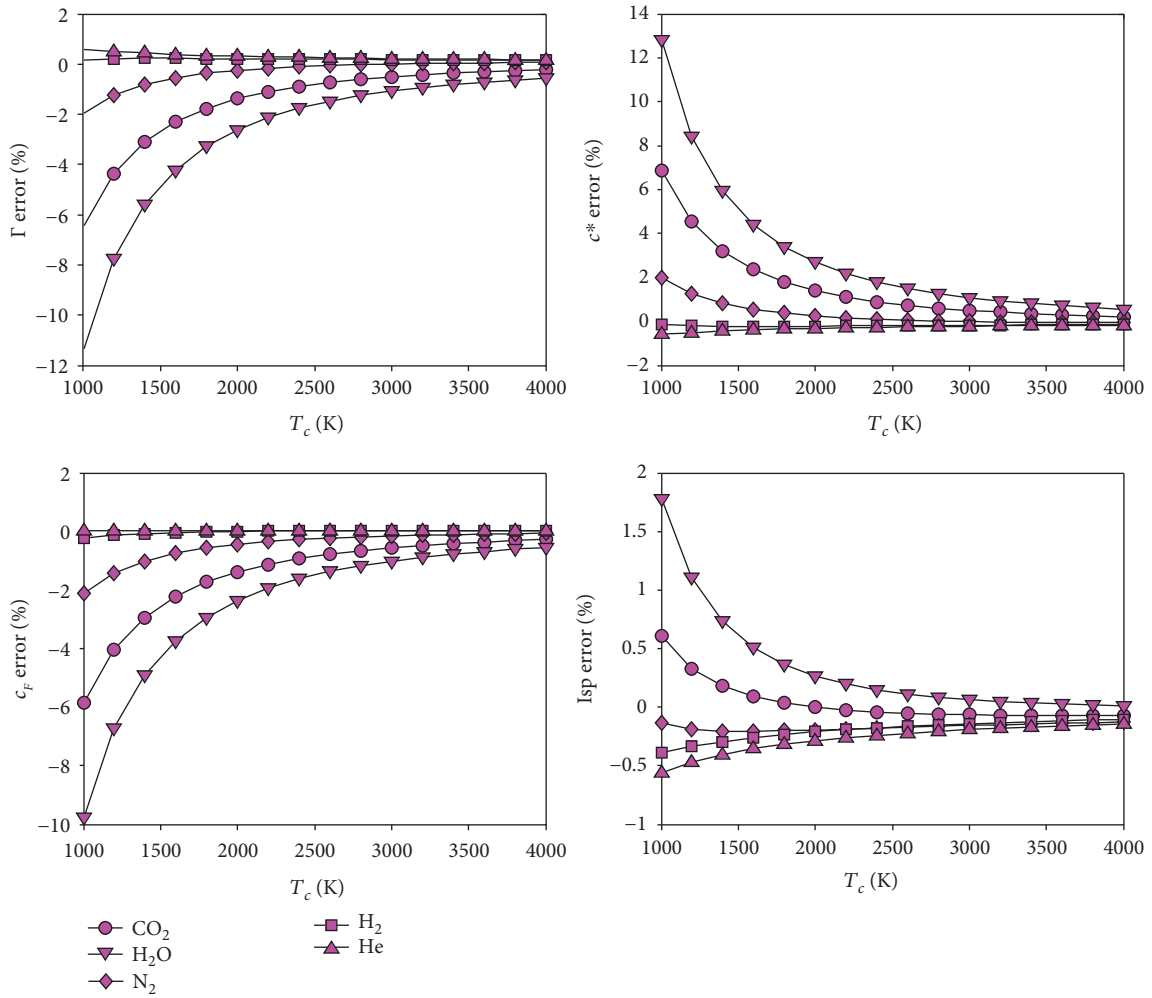

Figure 2: Errors of propulsion parameters of thermally perfect ideal gases with respect to VDW gases at different chamber temperatures, for vacuum expansion, $A_e/A_t = 100$ and $P_c = 10$ MPa.

Figure 1 depicts percent errors of propulsion parameters of calorically perfect ideal gases (CP-IG), assuming $P_c = 10$ MPa, chamber temperatures $T_c = 1000$ K–4000 K, and frozen flow expansion in vacuum for $A_e/A_t = 100$. Table 3 shows the maximum and minimum percent error values of propulsion and some flow thermodynamic parameters for CP-IG.

As seen in Figure 1, critical flow constant errors of N_2, H_2O, and CO_2 (CP-IG) have negative values and their

Table 4: Maximum and minimum error values of propulsion and flow parameters of thermally perfect ideal gases for P_c = 10 MPa, T_c = 1000 K–4000 K and frozen flow expansion in vacuum with A_e/A_t = 100.

ϕ	ε_{max} (%)					ε_{min} (%)				
	CO_2	H_2O	N_2	H_2	He	CO_2	H_2O	N_2	H_2	He
Γ	−0.212	−0.556	0.065	0.228	0.590	−6.428	−11.358	−1.966	0.142	0.165
c^*	6.870	12.813	2.006	−0.142	−0.165	0.213	0.559	−0.065	−0.227	−0.587
c_F	−0.284	−0.546	−0.062	0.038	0.034	−5.857	−9.782	−2.097	−0.230	0.020
Isp	0.610	1.778	−0.127	−0.104	−0.144	−0.071	0.010	−0.206	−0.388	−0.560
P_e	8.413	6.401	3.606	1.850	2.067	1.343	1.472	0.740	0.411	0.456
M_e	−0.248	−0.187	−0.252	−0.170	−0.236	−1.121	−0.529	−0.946	−0.800	−0.966
P_t	0.413	0.134	0.967	0.794	0.844	0.242	−0.394	0.274	0.196	0.213
T_t	0.305	0.430	0.370	0.243	0.339	0.046	0.041	0.068	0.044	0.085

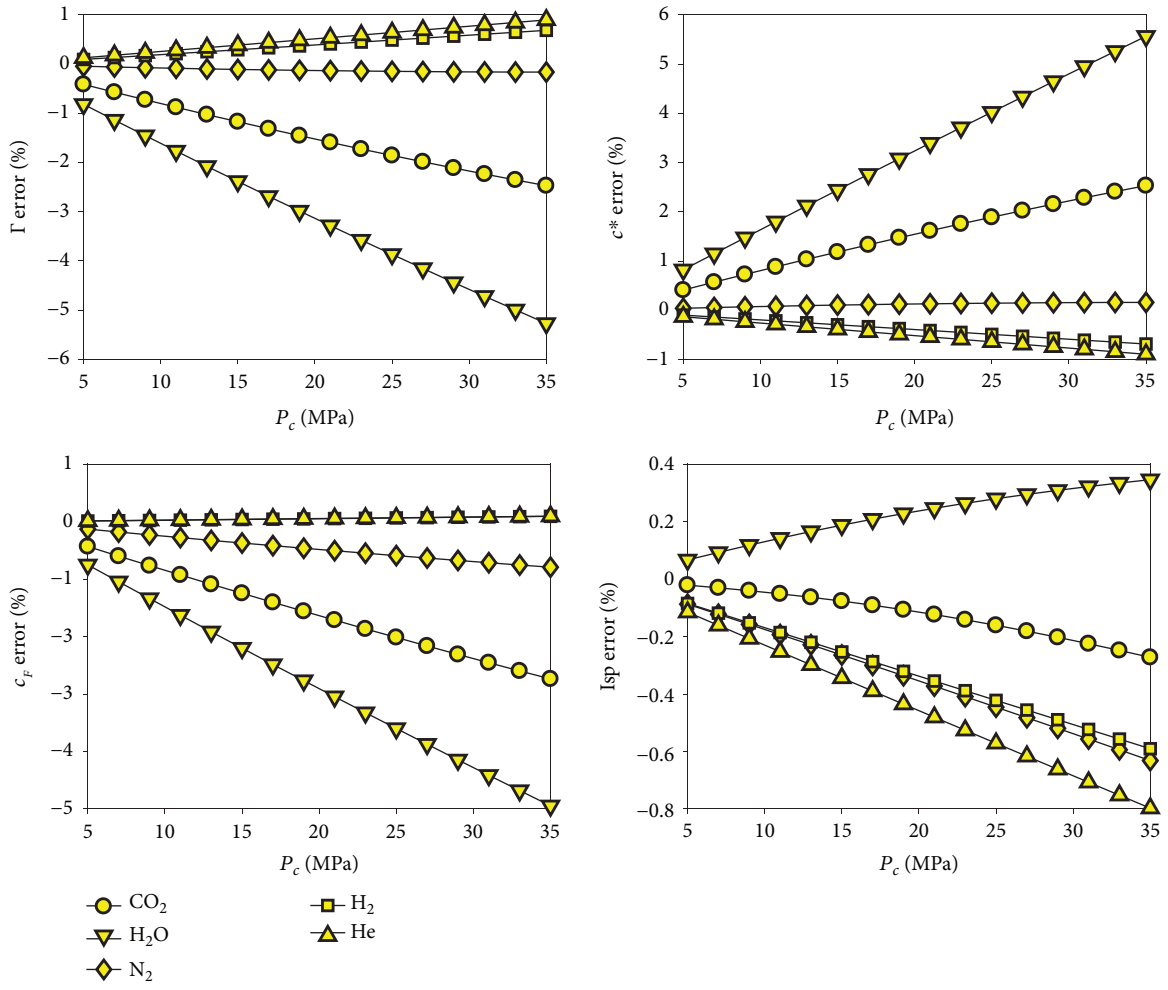

Figure 3: Errors of propulsion parameters of thermally perfect ideal gases with respect to VDW gases versus chamber pressures, for vacuum expansion, A_e/A_t = 100 and T_c = 2500 K.

absolute values decrease monotonically from 1000 K to 4000 K, while Γ errors of H_2 (CP-IG) are approximately zero and Γ errors of He are slightly positive and approach zero for larger temperatures. Characteristic velocity errors have similar values, but with opposite sign of the critical flow constant errors, since c^* varies inversely with Γ.

Thrust coefficient errors of H_2 and N_2 (CP-IG) are positive, and present maximum values of +3.14% at 2710 K and +1.87% at 1790 K, respectively, whereas the c_F error of He (CP-IG) is approximately zero along the temperature range considered. The c_F error of H_2O (CP-IG) is −7.07% at 1000 K and reaches a maximum of +0.87% at 2570 K,

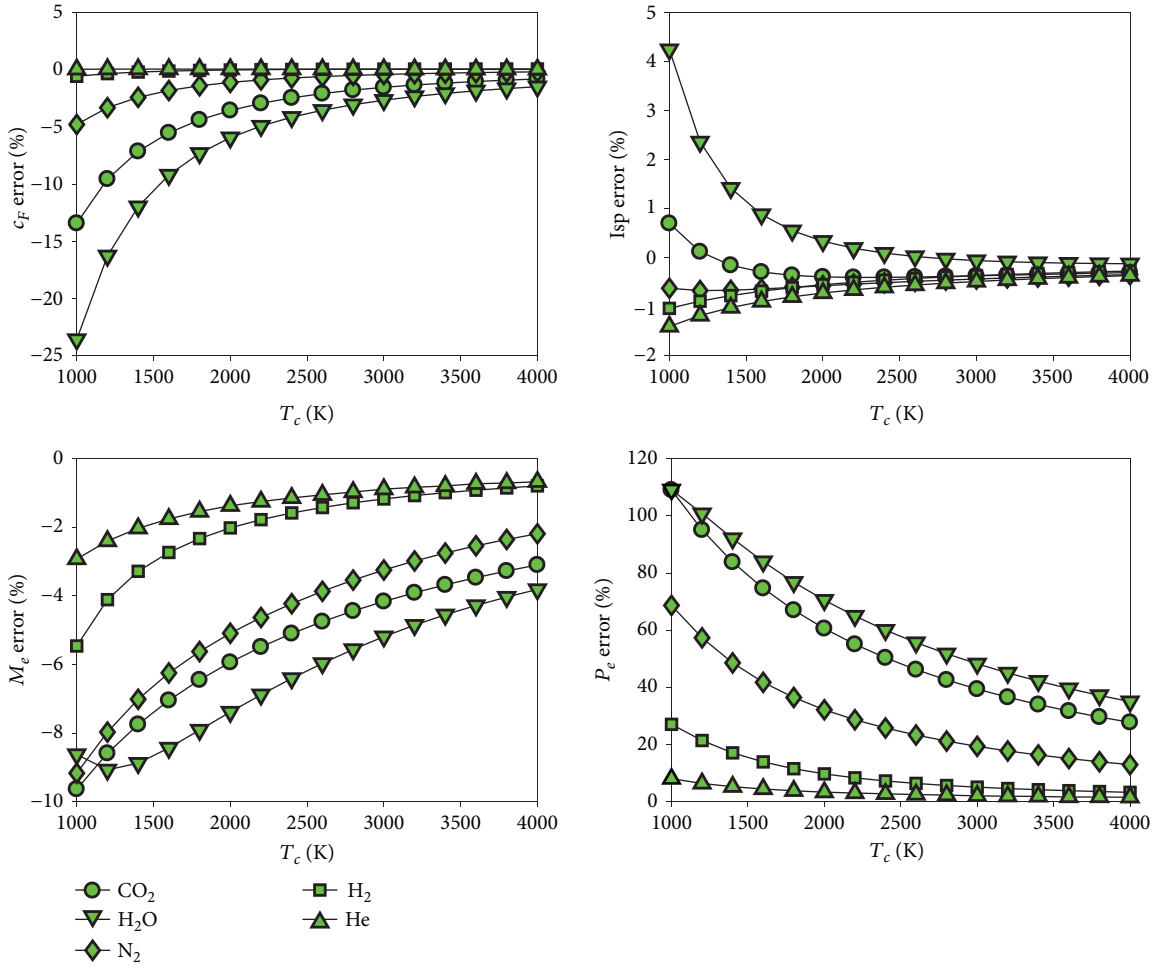

Figure 4: Errors of propulsion parameters and flow parameters of thermally perfect ideal gases with respect to VDW gases at different chamber temperatures, for vacuum expansion, $A_e/A_t = 50$ and $P_c = 25$ MPa.

whereas the c_F error of CO_2 (CP-IG) increases monotonically from −3.68% at 1000 K to +0.05% at 4000 K.

Isp errors of all CP ideal gases, except He, are positive within the temperature range considered. Isp errors of H_2 and N_2 (CP-IG) show maximum values of +3.11% at 2680 K and 2.61% at 1310 K, respectively, whereas Isp errors of H_2O and CO_2 (CP-IG) decrease monotonically from 5.03% to 1.2% and 3.01% to 0.28% from 1000 K to 4000 K. Isp errors of He (CP-IG) vary monotonically from −0.56% to −0.14% between 1000 K and 4000 K.

Exit pressure errors of CP ideal gases are positive and reach maximum values above 40%, except He that presents P_e errors less than 2.1%. Exit Mach number errors for all CP ideal gases are negative, and their absolute values are larger than 8%, except He that shows absolute values of M_e errors less than 1%. Errors of throat pressures and throat temperatures of all CP ideal gases are positive and reach maximum values lower than 1.5% and 0.8%, respectively.

Figure 2 depicts errors of propulsion parameters of thermally perfect ideal gases (TP-IG), assuming $P_c = 10$ MPa, $T_c = 1000$ K–4000 K, and frozen flow expansion in vacuum through a nozzle with $A_e/A_t = 100$. Table 4 presents the maximum and minimum error values of propulsion parameters and some flow parameters of TP ideal gases.

Critical flow constant errors of TP ideal gases are similar to critical flow constant errors of CP ideal gases. Γ errors of N_2, H_2, and CO_2 (TP-IG) have negative values, and their absolute values decrease monotonically from 1000 K to 4000 K, while Γ errors of H_2 (TP-IG) are approximately zero and Γ errors of He (TP-IG) are slightly positive and approach zero for larger temperatures. Characteristic velocity errors have opposite sign and are similar to the critical flow constant errors. H_2O (TP-IG) presents the largest c^* errors which vary from about +12.81% to 0.56% between 1000 K and 4000 K.

Properties of He (TP-IG) and He (CP-IG) are equal since specific heats of helium do not vary with temperature in the range considered.

Thrust coefficient errors of TP ideal gases show similar behavior to critical flow constants of TP ideal gases. Absolute values of c_F errors of H_2O, CO_2, and N_2 (TP-IG) decrease monotonically from 1000 K to 4000 K, whereas the values of c_F errors of H_2 and He (TP-IG) are approximately zero.

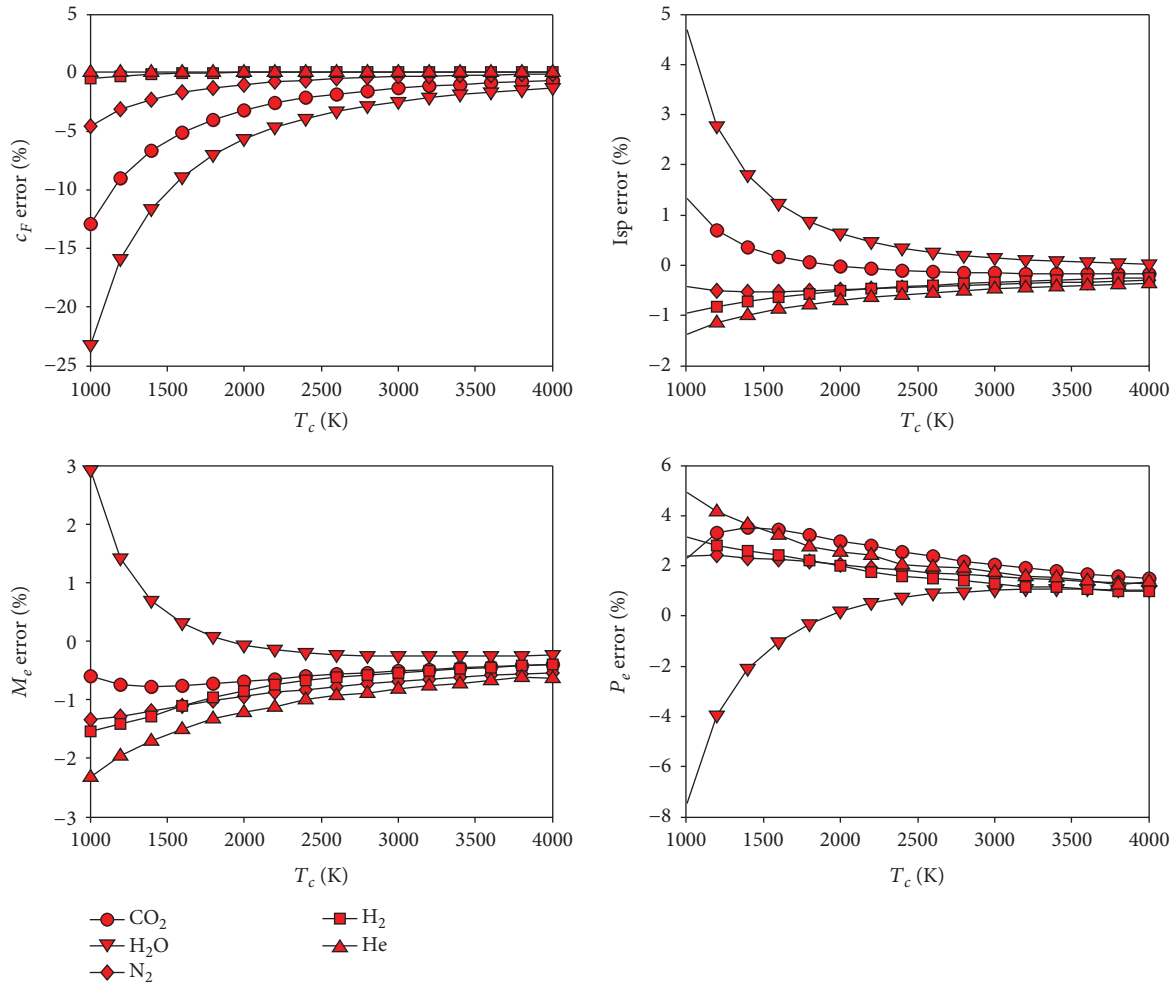

Figure 5: Errors of propulsion parameters and flow parameters of thermally perfect ideal gases with respect to VDW gases at different chamber temperatures, for vacuum expansion, $A_e/A_t = 200$ and $P_c = 25$ MPa.

Specific impulse errors of H_2O and CO_2 (TP-IG) decrease monotonically from +1.78% to 0.01% and from +0.61% to −0.07%, respectively, between 1000 K and 4000 K. Meanwhile, the absolute values of the Isp errors of H_2 and He (TP-IG) decrease monotonically from 0.39% to 0.10% and 0.56% to 0.14%, respectively, in the range considered. N_2 (TP-IG) presents a minimum Isp error of −0.21% at 1560 K.

Exit pressure errors of TP ideal gases are positive, decrease monotonically, and are significantly lower than exit pressure errors of CP ideal gases in the temperature range considered. The exception would be, again, helium, which presents equal values for TP and CP ideal gases.

Exit Mach number errors of the TP ideal gases considered are negative, and their absolute values are lower than the absolute values of the exit Mach number errors of CP ideal gases, except for helium which maintains the same values for TP and CP gases.

Throat pressure errors of TP ideal gases analyzed are positive, except H_2O (TP-IG) that shows negative errors up to 1500 K. Throat temperature errors of TP ideal gases analyzed are positive and decrease monotonically for increasing chamber temperatures.

Figure 3 presents the effects of pressures ($P_c = 5$ to 35 MPa) on percent errors of propulsion parameters of thermally perfect ideal gases in relation to van der Waals gases, for frozen vacuum expansion through a nozzle with area ratio 100, assuming $T_c = 2500$ K.

Despite being negative in many cases, the absolute values of the critical flow constant errors, characteristic velocity errors, and thrust coefficient errors of TP ideal gases increase approximately linearly with increasing chamber pressures for the temperature considered, since nonideal effects become more significant at higher pressures. Specific impulse errors of TP ideal gases are negative, except for H_2O, and show a slightly parabolic variation with increasing pressures. He (TP-IG) presents the largest absolute values of Isp errors, whereas H_2 and N_2 (TP-IG) present similar Isp behavior for the chamber temperature and chamber pressure range considered.

Figures 4 and 5 show errors of propulsion and flow parameters of thermally perfect ideal gases in relation to van der Waals gases, respectively, for flow expansion in vacuum through nozzles with area ratios 50 and 200, assuming a chamber pressure of 25 MPa and chamber temperatures 1000 K – 4000 K.

Thrust coefficient errors and specific impulse errors of TP ideal gases are not significantly affected by the nozzle area ratio variation, but their absolute values decrease significantly for increasing chamber temperatures. On the other hand, exit Mach number errors and exit pressure errors of TP ideal gases are strongly affected by the variation of a nozzle area ratio and their absolute values decrease monotonically with increasing temperatures, except for H_2O, which presents a minimum exit Mach number around 1200 K.

AGARD-AR-321 [16] presented experimental and theoretical data for the critical flow constant of air for pressures up to 40 atm, showing that errors of the calorically perfect solutions vary linearly with chamber stagnation pressures and inversely with chamber stagnation temperatures in the temperature and pressure ranges considered. Johnson [27] has presented numerical data, based on virial equation solutions, of the critical flow constants of N_2 and He, considering stagnation temperatures 100-400 K and stagnation pressures 0-300 atm. The N_2 critical flow constant error presented quite slight variations with increasing pressures, for temperatures approaching 400 K. In the case of He, the critical flow constants varied linearly with pressure in all temperatures considered. Similar tendencies have been observed in the present results for the critical flow constants, for both calorically and thermally perfect ideal gases compared to VDW gases.

5. Conclusions

Real gas effects and the variation of fluid properties can significantly affect propulsion parameters of rockets and thermodynamic parameters of nozzles. In general, the influence of real gas effects is more meaningful for lower chamber temperatures and higher chamber pressures. However, the flow through a nozzle presents large pressure and temperature variations which yield significant effects on exhaustion properties. New analytical solutions for propulsion parameters were derived, considering gases obeying the van der Waals equation of state and assuming specific heats varying accordingly to pressure and temperature. Equations for specific impulses, thrust coefficients, characteristic velocities, critical flow constants, and throat and exit properties were determined, considering one-dimensional isentropic frozen flows through a nozzle. Errors were calculated for the vacuum expansion of calorically perfect and thermally perfect ideal gases, in comparison to solutions for the expansion of van der Waals gases. Data were presented for He, H_2, N_2, H_2O, and CO_2, for chamber temperatures 1000-4000 K and chamber pressures 5-35 MPa, with different nozzle expansion ratios. Correction factors for the effects of real gases and variable properties, in general, are small; however, they can be larger than other correction factors usually adopted for design and performance analysis of real nozzles, depending on chamber conditions and propellant choice. Equations for the optimum thrust coefficients and optimum specific impulses were derived indicating the influences of covolumes and attraction parameters. Larger covolumes and smaller intermolecular forces increase the optimum specific impulse, disregarding the influences on specific heats and combustion temperature. Further analysis may consider mixtures of gases or combustion products, more accurate equations of state, equilibrium, and nonequilibrium flows, heat transfer, viscous losses, boundary layer formation, flow separation, presence of shock waves, and three-dimensional losses.

Nomenclature

Abbreviations

CEA: Chemical Equilibrium and Applications
CFD: Computational fluid dynamics
CP: Calorically perfect
EOS: Equation of state
IG: Ideal gases
NA: Noble-Abel
NASA: National Aeronautics and Space Administration
TP: Thermally perfect
VDW: van der Waals.

Symbols

A: Area (m^2)
a: Coefficient for intermolecular attraction ($Pa \cdot m^6 \cdot kg^{-2}$)
b: Covolume (m^3/kg)
b^*: Nondimensional covolume
c: Speed of sound ($m \cdot s^{-1}$)
c^*: Characteristic velocity ($m \cdot s^{-1}$)
c_F: Thrust coefficient
c_p: Specific heat at constant pressure ($J \cdot kg^{-1} \cdot K^{-1}$)
c_v: Specific heat at constant volume ($J \cdot kg^{-1} \cdot K^{-1}$)
F: Force, thrust (N)
g_o: Standard acceleration of gravity at sea level ($m \cdot s^{-2}$)
h: Enthalpy ($J \cdot mol^{-1} \cdot K^{-1}$)
Isp: Specific impulse (s^{-1})
$\dot{m}$: Mass flow rate ($kg \cdot s^{-1}$)
M: Mach number
P: Pressure (Pa)
R: Specific gas constant ($J \cdot kg^{-1} \cdot K^{-1}$)
s: Entropy ($J \cdot K^{-1}$)
T: Temperature (K)
u: Flow velocity ($m \cdot s^{-1}$)
v: Specific volume ($m^3 \cdot kg^{-1}$)
X: Molar fraction
ε: Nondimensional attraction parameter
$\varnothing$: Percent error
γ: Ratio of specific heats
Γ: Critical flow constant
ρ: Density ($kg \cdot m^{-3}$).

Subscripts

a: Ambient condition
c: Chamber condition
cr: Critical condition
e: Exit condition
i: Propellant/product
max: Maximum condition
s: Sound condition

t: Throat condition
opt: Optimum condition.

Superscripts

0: Ideal gas property.

Data Availability

No data were used to support this study.

Conflicts of Interest

The authors declare that there is no conflict of interest regarding the publication of this paper.

References

[1] G. C. Oates, Ed., *Aerothermodynamics of Gas Turbine and Rocket Propulsion*, AIAA Education Series, AIAA, New York, NY, USA, 1984.

[2] B. J. McBride and S. Gordon, *Computer program for calculation of complex chemical equilibrium compositions and applications*, II-User's Manual and Program Description, NASA RP-1331-P2, 1996.

[3] G. Yahiaoui and H. Olivier, "Development of a short-duration rocket nozzle flow simulation facility," *AIAA Journal*, vol. 53, no. 9, pp. 2713–2725, 2015.

[4] M. Naderi and L. Guozhu, "Static performance modeling and simulation of the staged combustion cycle LPREs," *Aerospace Science and Technology*, vol. 86, pp. 30–46, 2019.

[5] O. J. Haidn and M. Habiballah, "Research on high pressure cryogenic combustion," *Aerospace Science and Technology*, vol. 7, no. 6, pp. 473–491, 2003.

[6] K. M. Akyuzlu, "Numerical study of high-temperature and high-velocity gaseous hydrogen flow in a cooling channel of a nuclear thermal rocket core," *Journal of Nuclear Engineering and Radiation Science*, vol. 1, no. 4, article 041006, 2015.

[7] M. Marchionni, S. K. Aggarwal, I. K. Puri, and D. Lentini, "The influence of real-gas thermodynamics on simulations of freely propagating flames in methane/oxygen/inert mixtures," *Combustion Science and Technology*, vol. 179, no. 9, pp. 1777–1795, 2007.

[8] Z. Yue, R. Hessel, and R. D. Reitz, "Investigation of real gas effects on combustion and emissions in internal combustion engines and implications for development of chemical kinetics mechanisms," *International Journal of Engine Research*, vol. 19, no. 3, pp. 269–281, 2018.

[9] K. K. Wetzel and W. C. Solomont, "Hydrogen recombination kinetics and nuclear thermal rocket performance prediction," *Journal of Propulsion and Power*, vol. 10, no. 4, pp. 492–500, 1994.

[10] F. Petitpas and E. Daniel, "Compressible model for dilute flows," *AIAA Journal*, vol. 53, no. 8, pp. 2289–2299, 2015.

[11] M. Sellam and A. Chpoun, "Numerical simulation of reactive flows in overexpanded supersonic nozzle with film cooling," *International Journal of Aerospace Engineering*, vol. 2015, Article ID 252404, 15 pages, 2015.

[12] K. B. M. Q. Zaman, T. J. Bencic, A. F. Fagan, and M. M. Clem, "Shock-induced boundary-layer separation in round convergent–divergent nozzles," *AIAA Journal*, vol. 54, no. 2, pp. 434–442, 2016.

[13] A. Chaudhuri and A. Hadjadj, "Numerical investigations of transient nozzle flow separation," *Aerospace Science and Technology*, vol. 53, pp. 10–21, 2016.

[14] R. C. Johnson, "Real-gas effects in critical-flow-through nozzles and tabulated thermodynamic properties," NASA TN D-2565, 1965.

[15] D. W. Witte and K. E. Tatum, *Computer code for determination of thermally perfect gas properties*, 1994, NASA TP-3447.

[16] Annon, "Sonic nozzles for mass flow measurement and reference nozzles for thrust verification," AGARD-AR-321, 1997.

[17] J. H. Kim, H. D. Kim, T. Setoguchi, and S. Matsuo, "A computational study of real gas flows through a critical nozzle," *Proceedings of the Institution of Mechanical Engineers, Part C: Journal of Mechanical Engineering Science*, vol. 223, no. 3, pp. 617–626, 2009.

[18] D. A. Yoder, N. J. Georgiadis, and M. R. O'Gara, "Frozen chemistry effects on nozzle performance simulations," NASA TM-215507, 2009.

[19] J. Górski and S. Rabczak, "Critical flow of dense gases – modelling and experimental validation," *International Journal of Thermodynamics*, vol. 15, no. 1, pp. 27–33, 2012.

[20] J. Nagao, S. Matsuo, M. Mohammad, T. Setoguchi, and H. D. Kim, "Numerical study on characteristics of real gas flow through a critical nozzle," *International Journal of Turbo and Jet Engines*, vol. 29, no. 1, pp. 21–27, 2012.

[21] H. Ding, C. Wang, and Y. Zhao, "Flow characteristics of hydrogen gas through a critical nozzle," *International Journal of Hydrogen Energy*, vol. 39, no. 8, pp. 3947–3955, 2014.

[22] F. S. Costa, "Propulsion parameters of Noble-Abel gases," in *Procceedings of the 24th ABCM International Congress of Mechanical Engineering*, Curitiba, PR, Brazil, 2017.

[23] B. J. McBride, M. Zehe, and S. Gordon, "NASA Glenn coefficients for calculating thermodynamic properties of individual species," NASA TP-211556, 2002.

[24] E. W. Lemmon, M. O. McLinden, and D. G. Friend, "Thermophysical properties of fluid systems," in *NIST Chemistry Webbook: NIST Standard Reference Database Number 69*, P. J. Linstrom and W. G. Mallard, Eds., National Institute of Standards and Technology, Gaithersburg MD, USA, 2018.

[25] S. M. Walas, *Phase equilibria in chemical engineering*, Elsevier Ltd., Butterworth, MA, 1985.

[26] M. S. Cramer and R. Sen, "Exact solutions for sonic shocks in van der Waals gases," *Physics of Fluids*, vol. 30, no. 2, p. 377, 1987.

[27] R. C. Johnson, "Real-gas effects in critical flow through nozzles and thermodynamic properties of nitrogen and helium at pressures up to 300×10^5 newtons per square meter (approx. 300 atm)," NASA SP-3046, 1995.